



创业与管理学院

School of Entrepreneurship and Management

SHANGHAITECH SEM WORKING PAPER SERIES

No. 2022-001

An Infinite Hidden Markov Model with Stochastic Volatility

Chenxing Li

Center for Economics, Finance and Management Studies, Hunan University

John M. Maheu

DeGroote School of Business, McMaster University

Qiao Yang

School of Entrepreneurship and Management, ShanghaiTech University

March 29, 2022

<https://ssrn.com/abstract=4069359>

School of Entrepreneurship and Management

ShanghaiTech University

<http://sem.shanghaitech.edu.cn>

An Infinite Hidden Markov Model with Stochastic Volatility*

Chenxing Li[†]

John M. Maheu[‡]

Qiao Yang[§]

March 2022

Abstract

This paper extends the Bayesian semiparametric stochastic volatility (SV-DPM) model of Jensen and Maheu (2010). Instead of using a Dirichlet process mixture (DPM) to model return innovations, we use an infinite hidden Markov model (IHMM). This allows for time variation in the return density beyond that attributed to parametric latent volatility. The new model nests several special cases as well as the SV-DPM. We also discuss posterior and predictive density simulation methods for the model. Applied to equity returns, foreign exchange rates, oil price growth and industrial production growth, the new model improves density forecasts, compared to the SV-DPM, a stochastic volatility with Student-t innovations and other fat-tailed volatility models.

Keywords: stochastic volatility; Markov-switching; MCMC; Bayesian; nonparametric; semi-parametric

JEL codes: C58; C14; C32; C11; C34

*We are grateful for the helpful comments of seminar participants at the 2018 RECA Bayesian Econometric workshop, 2020 virtual SBIES, Tongji University, Hunan University, 2021 virtual CFE, 2021 virtual China Meeting of Econometrics Society. Maheu thanks the SSHRC of Canada for their financial support. Yang thanks the start-up fund of ShanghaiTech and the Young Scientists Fund of NSFC (Project 72103137) for their financial support.

[†]Center for Economics, Finance and Management Studies, Hunan University. Email:lichenxing@hnu.edu.cn

[‡]DeGroote School of Business, McMaster University. Email:maheujm@mcmaster.ca

[§]Corresponding author: School of Entrepreneurship and Management, ShanghaiTech University, China. Email: yangqiao@shanghaitech.edu.cn

1 Introduction

Changing volatility has become ubiquitous in economic time-series data. Besides high frequency asset returns, conditional heteroskedasticity is even found in lower frequency macroeconomic aggregate data (Chan, 2013, 2017; Marcellino et al., 2016; Diebold et al., 2017; Carriero et al., 2019). Generalized autoregressive conditional heteroskedasticity (GARCH, Bollerslev, 1986) and stochastic volatility (SV, Taylor, 1982), are popular modelling approaches used to capture volatility dynamics. However, much less attention has been paid to modelling unknown return innovation distributions.

Flexible modelling of return innovations coupled with parametric volatility models can be found in the work of Jensen and Maheu (2010), Delatola and Griffin (2011, 2013), Kalli et al. (2013) and Liu (2020). Although flexible, these approaches assume that the underlying innovation distribution is constant over time. Volatility changes from the parametric portion of the model, but the underlying return distribution is fixed over time.

This paper explores an SV parametric specification, coupled with an infinite hidden Markov component that governs a mixture of normals. This is a direct extension to Jensen and Maheu (2010) and replaces the Dirichlet process mixture (DPM) with a Markov mixture model. The Markov chain allows for the possibility that the weights on the mixture change over time. In theory this means that the mixture can capture changing conditional skewness, kurtosis as well as changes in tail dynamics beyond what the SV component can account for.

The infinite hidden Markov model (IHMM) has been fruitfully used in other settings: GARCH modelling (Dufays, 2016), inflation dynamics (Song, 2014; Jochmann, 2015) short-term interest rates (Maheu and Yang, 2016), realized covariance models (Jin and Maheu, 2016; Jin et al., 2019), macroeconomic forecasting (Hou, 2017; Yang, 2019) and model combination (Jin et al., 2021).

The IHMM approximates the unknown conditional return distribution that is nonparametrically similar to the DPM. Unlike the DPM model, the mixture weights in the IHMM are Markovian. The prior on this Markov chain is constructed using two layers of nested Dirichlet processes called a hierarchical Dirichlet process (Teh et al., 2006). The IHMM can be seen as a regime-switching model with an infinite number of states. In each period, the return distribution is approximated by an infinite mixture and the mixture weights depend on the previous state the system is in. In contrast, the DPM approximates the unknown distribution with an infinite mixture, but the weights are constant and independent of previous states.

Due to the unbounded state space, the IHMM can accommodate both structural breaks and recurrent changes in a unified framework. However, a regime switching model may not

be able to capture the strong persistence in the volatility dynamics (Ryden et al., 1998). Our model’s SV component captures this and allows the IHMM component to focus on local changes in the shape of the unknown distributions.

Our model can also be seen as an extension of Virbickaitė and Lopes (2018) which has a two-state Markov switching process that affects the conditional mean of the log-volatility, while the return innovations are nonparametrically modelled. Related work that includes discrete parameter changes in volatility modelling are Maheu and McCurdy (2000), Calvet and Fisher (2004), Griffin and Steel (2011) and Bauwens et al. (2014).

Posterior simulation relies on Markov chain Monte Carlo (MCMC) methods. Posterior simulation for the IHMM component comes from Teh et al. (2006) and Maheu and Yang (2016); while the latent stochastic volatility is simulated with the random block sampler of Jensen and Maheu (2010). We apply the model to several different asset classes and compare it with a number of strong benchmark models, including the SV-DPM from Jensen and Maheu (2010) and SV model with Student-t innovations. While the SV component of the model captures movements that display strong persistence in volatility, the variance component directed from the IHMM portion can be thought of as capturing local changes in the long-run volatility.

Evaluating the model through predictive likelihood shows that the SV-IHMM is preferred to all other benchmarks. Predictive density plots indicate that the SV-IHMM tends to produce distributions with the fattest tails, when necessary.

This paper is organized as follows. Section 2 to 6 illustrate the specification of the proposed SV-IHMM, along with the sampling algorithm and density forecast computation. Section 7 describes the details of the return series used to test this model. Section 8 presents the posterior estimations of the SV-IHMM and three benchmark models. Section 9 further analyses our model’s out-of-sample performance compared with multiple benchmark models. Section 10 tests the robustness of the estimates and forecasts under different prior settings for hyper-parameters. Section 11 concludes. An Appendix details the posterior simulation methods used for our model.

2 The Model

Our proposed SV-IHMM model includes a parametric SV component, and a Bayesian non-parametric portion, following an infinite hidden Markov model (IHMM). The IHMM is constructed from the hierarchical Dirichlet process (HDP) introduced by Teh et al. (2006). The

hierarchical representation of the SV-IHMM is

$$\Gamma \sim \text{Stick}(\eta), \quad \Pi_j \stackrel{iid}{\sim} \text{Stick2}(\alpha, \Gamma), \quad j = 1, \dots, \infty, \quad (1a)$$

$$s_t | s_{t-1} \sim \Pi_{s_{t-1}}, \quad (1b)$$

$$r_t | s_t, h_t, \theta \sim N(\mu_{s_t}, \omega_{s_t}^2 \exp(h_t)), \quad (1c)$$

$$h_t | h_{t-1} \sim N(\phi h_{t-1}, \sigma_v^2), \quad (1d)$$

$$\theta_j \stackrel{iid}{\sim} \mathcal{H}, \quad j = 1, \dots, \infty, \quad (1e)$$

for $t = 1, \dots, T$. $\theta_{s_t} = \{\mu_{s_t}, \omega_{s_t}\}$ and $\theta = \{\theta_1, \theta_2, \dots\}$ is the collection of the state-dependent parameter vectors that are generated from the base measure \mathcal{H} . $s_t \in \{1, \dots, \infty\}$ is the state variable that is governed by the first-order Markov chain of infinite dimension with transition matrix Π . $\text{Stick}(\eta)$ and $\text{Stick2}(\alpha, \Gamma)$ are stick-breaking representations of the Dirichlet processes (Sethuraman, 1994; Teh et al., 2006). Let $\Gamma = \{\gamma_1, \dots, \gamma_\infty\}$ then $\Gamma \sim \text{Stick}(\eta)$ denotes a discrete distribution with weights generated as

$$\gamma_j = v_j \prod_{l=1}^{j-1} (1 - v_l), \quad v_j \stackrel{iid}{\sim} \text{Beta}(1, \eta), \quad j = 1, 2, 3, \dots \quad (2)$$

Γ serves as a centering distribution with support on the natural numbers. Each row of Π is drawn as $\Pi_j \sim \text{Stick2}(\alpha, \Gamma)$. The distribution of Π_j has weights generated as

$$\pi_{ji} = \hat{\pi}_{ji} \prod_{l=1}^{i-1} (1 - \hat{\pi}_{jl}), \quad \hat{\pi}_{ji} \stackrel{iid}{\sim} \text{Beta} \left(\alpha \gamma_i, \alpha \left(1 - \sum_{l=1}^i \gamma_l \right) \right), \quad (3)$$

where π_{ji} is an element of Π at the j th row and i th column. π_{ji} represents the probability of moving from parameter θ_j to parameter θ_i .

η and α are concentration parameters that govern the likelihood of new states occurring when the model is applied to a finite dataset. The two DP's in (1a) are linked by sharing the same atom θ . This means that each draw of Π_j has the same support and facilitates the construction of an infinite transition matrix that can be used to govern s_t . $\text{Stick}(\eta)$ determines the top-level hierarchy and is shared in the second level. The second layer, $\text{Stick2}(\alpha, \Gamma)$, governs each row of the transition matrix and is centered such that $E[\Pi_j] = \Gamma$. The IHMM nests the Dirichlet process mixture model of Antoniak (1974) when $\alpha \rightarrow 0$, and each row of the transition matrix converges to the same vector Γ .

The associated stick-breaking representation of the model is

$$p(r_t|\theta, \Pi, s_{t-1}, h_t) = \sum_{k=1}^{\infty} \pi_{s_{t-1}k} N(r_t; \mu_k, \omega_k^2 \exp(h_t)), \quad (4a)$$

$$h_t = \phi h_{t-1} + \sigma_v v_t, \quad v_t \sim N(0, 1), \quad (4b)$$

where $N(r_t; \mu_k, \omega_k^2 \exp(h_t))$ denotes the normal density function with mean μ_k , and variance $\omega_k^2 \exp(h_t)$ evaluated at r_t . $\pi_{s_{t-1}k}$ governs the weight assignments to different normal kernels, where the weights change accordingly over time via the first-order Markov chain. The model in (4) becomes the SV-DPM specification of Jensen and Maheu (2010) if the weights are independent of the previous state, where $\pi_{jk} = \pi_k$ for all j and k .

As in conventional SV models, the persistence in the volatility dynamics is captured through the lag term ϕh_{t-1} . The SV-IHMM has a second channel for persistence through the Markov chain which itself allows for persistence in the conditional mean μ_{s_t} , and the conditional variance component $\omega_{s_t}^2$. Since the long-run value of h_t is zero when $|\phi| < 1$, the parameter $\omega_{s_t}^2$ effectively controls and allows for local changes in the long-run variance of the returns. This is seen by rewriting the model as

$$r_t = \mu_{s_t} + \exp(h'_t/2) z_t \quad (5a)$$

$$h'_t - \log \omega_{s_t}^2 = \phi(h'_{t-1} - \log \omega_{s_{t-1}}^2) + \sigma_v v_t, \quad (5b)$$

where $h'_t = h_t + \log \omega_{s_t}^2$. Here the long-run mean of h'_t is $\log \omega_{s_t}^2$ and remains constant without any state change. State changes allow for both the conditional mean and the long-run mean of h'_t to change over time through $\omega_{s_t}^2$.

3 Benchmark Models

We consider the following benchmark models for comparison. The GARCH-N is defined as:

$$r_t = \mu + \sigma_t \epsilon_t, \quad \epsilon_t \sim N(0, 1), \quad \sigma_t^2 = \beta_0 + \beta_1(r_{t-1} - \mu)^2 + \beta_2 \sigma_{t-1}^2. \quad (6)$$

The GARCH-t replaces the normal distribution with a Student-t distribution:

$$r_t = \mu + \sigma_t u_t, \quad u_t \sim t(\nu), \quad \sigma_t^2 = \beta_0 + \beta_1(r_{t-1} - \mu)^2 + \beta_2 \sigma_{t-1}^2, \quad (7)$$

where $t(\nu)$ denotes a Student-t distribution with mean 0, scale parameter 1 and degree of freedom ν . The SV parametric versions, including the SV-N, are defined as:

$$r_t = \mu + \exp(h_t/2) \epsilon_t, \quad \epsilon_t \sim N(0, 1), \quad h_t = \xi + \phi h_{t-1} + \sigma_v v_t. \quad (8)$$

Similarly, SV-t has the following Student-t return innovations:

$$r_t = \mu + \exp(h_t/2) u_t, \quad u_t \sim t(\nu), \quad h_t = \xi + \phi h_{t-1} + \sigma_v v_t. \quad (9)$$

The SV-IHMM nests several models of interest that we can compare our model to. The first is an IHMM without the SV component. If $\sigma_v = 0$, and $h_t = 0, \forall t$ in the SV-IHMM then we have the IHMM:

$$\Gamma \sim \text{Stick}(\eta), \quad \Pi_j \stackrel{iid}{\sim} \text{Stick2}(\alpha, \Gamma), \quad j = 1, \dots, \infty, \quad (10a)$$

$$s_t | s_{t-1} \sim \Pi_{s_{t-1}}, \quad (10b)$$

$$r_t | s_t, h_t, \theta \sim N(\mu_{s_t}, \omega_{s_t}^2), \quad (10c)$$

$$\theta_j \stackrel{iid}{\sim} \mathcal{H}, \quad j = 1, \dots, \infty, \quad (10d)$$

As mentioned above, the infinite hidden Markov chain nests the DPM as a special case and, therefore, the SV-IHMM nests the SV-DPM of Jensen and Maheu (2010). The SV-DPM model is obtained by replacing the first two lines in (1a)–(1b) with

$$\Gamma \sim \text{Stick}(\eta), \quad (11a)$$

$$s_t \sim \Gamma, \quad t = 1, \dots, T. \quad (11b)$$

Finally, since the SV-IHMM nests the SV-DPM as in Jensen and Maheu (2010), it also nests the SV-t under certain parameter restrictions and prior assumptions.

4 Priors and Hierarchical Priors

This section defines the priors and hierarchical priors for the SV-IHMM and the benchmark models. Priors for the infinite Markov transition matrix Π are formed by $\text{Stick}(\eta)$ and $\text{Stick2}(\alpha, \Gamma)$, which were discussed in previous section. In order to minimize the impact of the prior, rather than fixing η and α , we follow Fox et al. (2011) and impose the hyper prior:

$$\eta \sim \text{Gamma}(2, 8), \quad \alpha \sim \text{Gamma}(2, 8), \quad E(\eta) = E(\alpha) = 0.25. \quad (12)$$

\mathcal{H} is the common base measure of the second layer of the DP's in the model. This prior is specified as $\mu_j \sim N(b_0, B_0)$ and $\omega_j \sim IG(\nu_0, s_0)$. Motivated by Song (2014), a hierarchical prior is used to learn from the data about these prior settings. These are

$$b_0 \sim N(0, 1), \quad B_0 \sim IW(3, I), \quad v_0 \sim Exp(1), \quad s_0 \sim Gamma(5, 1), \quad (13)$$

where I is an identity matrix, and $B_0 \sim IW(4, I)$ if the conditional mean is an AR(1) process. When a new state is introduced to the model, the associated draws of a new μ and ω are obtained from the informative priors that were influenced by data. This can contribute to faster learning about new states and, thus, improve the forecasts.¹ $\phi \sim N(0, 1)$ is truncated to the stationary region for an AR(1) process and $\sigma_v^2 \sim IG(11, 0.01)$.²

The prior and the hierarchical prior of the IHMM are the same as that of the SV-IHMM. For the SV-DPM, we keep same priors, hyper-priors and hierarchical priors as in SV-IHMM. The key difference is that there is only one concentration parameter, $\eta \sim Gamma(2, 8)$, in SV-DPM. Let $\mu, \beta_0, \beta_1, \beta_2$ follow an independent $N(0, 1)$ in GARCH-N and GARCH-t. Similarly, μ, ξ, ρ follow an independent $N(0, 1)$ and $\sigma_v^2 \sim IG(11, 0.01)$ in both the SV-N and SV-t.² The prior for ν in Student-t is uniform: $\nu \sim U[2, 50]$.

5 Posterior Sampling

The sampling scheme for the SV-IHMM consists of two parts. First, we sample the state-dependent parameters, transition matrix, latent states and the concentration parameters of the HDP. Second, we sample the log-volatility.

Conditional on the log-volatility, the sampling algorithm for the state-dependent parameters is similar to that of the IHMM. We use the beam sampler from Van Gael et al. (2008). This randomly generates the auxiliary variables (slices) that stochastically truncate the infinitely dimensional transition matrix Π into a finite size so that the forward-filtering backward-sampling (FFBS, Chib, 1996) can be applied.

We define an auxiliary variable $u_t > 0$ (slice) that is generated by a uniform density as follows:

$$p(u_t | s_t, s_{t-1}, \Pi,) = \frac{\mathbb{1}(u_t < \pi_{s_{t-1}, s_t})}{\pi_{s_{t-1}, s_t}} \quad t = 1, \dots, T, \quad (14)$$

where $\mathbb{1}(\cdot)$ denotes the indicator function. Augmenting the model with u_t gives us the

¹Maheu and Yang (2016) documents significant improvements in the density forecast accuracy.

²We apply a very informative prior to separately identify the SV and IHMM components. A prior of $\sigma_v^2 \sim IG(5, 0.25)$ provides similar forecast results.

following target density:

$$p(r_t, u_t | \theta, \Pi, s_{t-1}, h_t) = \sum_{k=1}^{\infty} \mathbb{1}(u_t > \pi_{s_{t-1}k}) N(r_t; \mu_k, \omega_k^2 \exp(h_t)). \quad (15a)$$

Integrating out the slice yields (4a), but given u_t there are now a finite number of non-zero terms $\mathbb{1}(u_t > \pi_{s_{t-1}k})$, that we need to account for. This is easily achieved by defining K to satisfy $\max_{i \in \{1, \dots, K\}} \{1 - \sum_{j=1}^K \pi_{i,j}\} < \min_{t \in \{1, \dots, T\}} \{u_t\}$.

Now, sampling the states and the state-dependent parameters is done on a finite Markov switching model. In each iteration, of the posterior sample K will change.

The FFBS within the Beam sampler is applied in the following way:

The prediction step for $k = 1, \dots, K$ calculates as

$$p(s_t = k | u_{1:T}, \Pi, r_{1:t-1}) \propto \sum_{j=1}^K \mathbb{1}(u_t < \pi_{j,k}) p(s_{t-1} = j | u_{1:T}, \Pi, r_{1:t-1}, h_t). \quad (16)$$

The update step for $k = 1, \dots, K$ calculates as

$$p(s_t = k | u_{1:T}, \Pi, r_{1:t}) \propto p(s_t = k | u_{1:T}, \Pi, r_{1:t-1}) p(r_t | r_{1:t-1}, \mu_k, \omega_k, h_t). \quad (17)$$

After $s_{1:T}$ are sampled, we update K by excluding the states for which there are no observation assignment. The slices are drawn from the uniform distribution.

To sample h_t , a random length block-move Metropolis-Hastings (MH) sampler of Jensen and Maheu (2010) is used. The block size of this sampler is randomly drawn from a Poisson distribution with preset hyperparameter λ_h , and the expected block size is $\lambda_h + 1$. Once h_t is sampled, θ and σ_v can be easily sampled via conjugacy. $c_{1:K}$ represents the oracle counts that helps us sample α and η . Appendix A describes the details of each sampling step. All of the posterior steps are summarized in the following:

$$\begin{array}{lll} p(u_{1:T} | s_{1:T}, \Pi) & p(s_{1:T} | \Pi, u_{1:T}, r_{1:T}, h_{1:T}, \theta) & p(c_{1:K} | s_{1:T}, \Gamma, \alpha) \\ p(\Gamma | s_{1:T}, \eta, \alpha, c_{1:K}) & p(\Pi | s_{1:T}, \Gamma, \alpha, c_{1:K}) & p(\mu_{1:K}, \omega_{1:K} | r_{1:T}, s_{1:T}) \\ p(\alpha, \eta | s_{1:T}, c_{1:K}) & p(h_{1:T} | h_{1:T}, r_{1:T}, \theta) & p(\phi | h_{1:T}, \sigma_v) \end{array}$$

Let $\Theta = \{\mu_{1:K}, \omega_{1:K}, \phi, \sigma_v, h_{1:T}\}$. Sampling each of the conditional posterior distributions provides one iteration of the sampler. After dropping the burn-in draws, the posterior average

or quantiles of each parameter of interest are computed from N draws. For example,

$$E(\mu_{s_t}|r_{1:T}) = \frac{1}{N} \sum_{i=1}^N \mu_{s_t}^{(i)} \text{ for } t = 1, \dots, T \quad (19)$$

is the posterior mean of μ_{s_t} at each point in time.

6 Density Forecasts

The predictive distribution of returns integrates out all of the parameter uncertainty and has the following generic form:

$$p(r_{t+1}|r_{1:t}) = \int p(r_{t+1}|\Theta, r_{1:t})p(\Theta|r_{1:t})d\Theta \quad (20)$$

where $p(r_{t+1}|\Theta, r_{1:t})$, is the density of r_{t+1} given the parameter set Θ and the past returns. $p(\Theta|r_{1:t})$ is the posterior density of Θ , given the data. Any feature of the predictive density, such as the predictive mean, can be obtained through simulation methods.

A central component in a Bayesian model comparison is the predictive likelihood. This is obtained for a model by evaluating the predictive density at the realized data point r_{t+1} . The predictive likelihood measures the accuracy of the density forecasts, with larger values being better.

To compute the log-predictive likelihood (LPL) for the SV-IHMM, we do the following: Given the posterior draws from each iteration of the MCMC sampler $\{\mu_{s_t}^{(i)}, \omega_{s_t}^{(i)}, \Pi^{(i)}, s_t^{(i)}, \phi_h^{(i)}, \sigma_v^{(i)}, h_t^{(i)}\}$, we draw $s_{t+1}^{(i)} \in \{1, \dots, K^{(i)} + 1\}$, where $K^{(i)}$ is the total number of active states:

1. Simulate the state variable $s_{t+1}^{(i)}$ through $\Pi_{s_T}^{(i)}$, conditional on $s_t^{(i)}$.
2. If $s_{t+1}^{(i)} \leq K^{(i)}$, then r_{t+1} is assigned to an existing state, with state-dependent parameter $\theta_{s_{t+1}} = (\mu_{s_{t+1}}^{(i)}, \omega_{s_{t+1}}^{(i)})$. Otherwise, r_{t+1} is assigned to a new state, $s_{t+1} = K^{(i)} + 1$, where $(\mu_{s_{t+1}}^{(i)}, \omega_{s_{t+1}}^{(i)})$ is drawn from the hierarchical prior, $\mu_{s_{t+1}} \sim N(b_0, B_0)$ and $\omega_{s_{t+1}}^2 \sim IG(\nu_0, s_0)$.

If N is the total number of MCMC draws used for the forecasting inference, then the predictive likelihood at $t + 1$ is computed over all MCMC draws:

$$p(r_{t+1}|r_{1:t}) \approx \frac{1}{N} \sum_{i=1}^N p(r_{t+1}|\mu_{s_{t+1}}^{(i)}, \omega_{s_{t+1}}^{(i)2} \exp(h_{t+1}^{(i)})), \quad (21)$$

where $p(r_{t+1}|\mu_{s_{t+1}}^{(i)}, \omega_{s_{t+1}}^{(i)2} \exp(h_{t+1}^{(i)}))$ denotes the normal density evaluated at r_{t+1} with mean

$\mu_{s_{t+1}}^{(i)}$ and variance $\omega_{s_{t+1}}^{(i)2} \exp(h_{t+1}^{(i)})$. $h_{t+1}^{(i)}$ is obtained by simulating forward a value from the existing MCMC draw $h_{t+1}^{(i)} \sim N(\phi^{(i)} h_t^{(i)}, \sigma_v^{(i)2})$.

Equation (21) measures the predictive likelihood of forecast accuracy at period $t + 1$. The forecast performance over the entire out-of-sample period, t_0, \dots, t_1 $t_0 \leq t_1$, is determined by computing the joint predictive likelihood of model \mathcal{M}_A in the following way:

$$LPL_A = \log p(r_{t_0:t_1} | r_{1:t_0}, \mathcal{M}_A) = \sum_{t=t_0}^{t_1} \log p(r_t | r_{1:t-1}, \mathcal{M}_A) \quad (22)$$

Two models, \mathcal{M}_A and \mathcal{M}_B , can be compared with a log-predictive Bayes factor (BF) defined as $BF_{AB} = LPL_A - LPL_B$. Positive values favour \mathcal{M}_A . Values above 5 are regarded as strong evidence for \mathcal{M}_A .

The root mean squared forecast error (RMSFE) for \mathcal{M}_A is computed in a similar way:

$$\text{RMSFE} = \sqrt{\frac{\sum_{t=t_0}^{t_1} (r_t - E(r_t | r_{1:t-1}, \mathcal{M}_A))^2}{t_1 - t_0 + 1}}, \quad (23)$$

where $E(r_t | r_{1:t-1}, \mathcal{M}_A)$ is the predictive mean for r_t given data $r_{1:t-1}$. For each out-of-sample period, we re-estimate the model to compute the predictive quantities.

7 Data

Four time series datasets are studied using the SV-IHMM and the benchmark models. These datasets cover an equity, a commodity, a foreign exchange rate and a macroeconomic indicator. We select Apple Inc. (AAPL) as a large cap equity and use its common stock returns at daily frequencies, dated from December 15th, 1980 to December 31, 2020, and obtain a sample size of 10,099, which we retrieved from the CRSP.³ For the foreign exchange rate, we study the daily exchange rates of the Canadian against the US dollar for the period January 5th, 1971, to December 31, 2020 (12,057 observations), which we obtained from the FRED.⁴ West Texas Intermediate (WTI) crude oil spot free on board (FOB) prices are selected for our commodity prices and run from January 2, 1986 to December 31, 2020. There are 8,819 daily observations and these are downloaded from the U.S. Energy Information Administration. The U.S. industrial production index is downloaded from FRED and is a monthly measure of real output. There are 1,222 observations, dating from March, 1919 to December, 2020. All of the time series are transformed into rates of change by taking the log difference and

³Center for Research in Security Prices.

⁴Federal Reserve Economic Data, U.S. Federal Reserve Bank of St. Louis.

scaling it by 100. The data series are labelled AAPL, USD/CAD, Crude Oil and IP Growth, respectively. Table 1 illustrates some descriptive statistics of the data. AAPL and Crude Oil have greater volatility and skewness than USD/CAD and IP Growth.

8 Posterior Analysis

Table 2 summarizes the posterior parameter estimates of only the most competitive models: the SV-IHMM, SV-DPM, SV-t and GARCH-t across the four datasets. The posterior means and 0.95 density interval estimates are reported. The burn-in MCMC draws are 20,000 and another $N = 20,000$ draws are used for the posterior inferences. In the case of IP Growth, we include an AR(1) term with a fixed coefficient in the conditional mean and denote it as ρ in the table. In the nonparametric models ρ is also state dependent along with the intercept.

First, introducing a second dynamic structure on the volatility through $\omega_{s_t}^2$ does not weaken the volatility persistence of h_t . For instance, ϕ is in the range of 0.993 – 0.999 for all of the models. Second, in the nonparametric components, we find that the SV-IHMM model uses more active states than the SV-DPM in applications of AAPL and USD/CAD, whereas it is about the same in application of Crude Oil and IP Growth, as shown in Table 2. The posterior mean of K is larger and the density interval shift rightward in the SV-IHMM, compared to the SV-DPM, for AAPL and USD/CAD. This can be seen in Figure 1.

The estimates for the SV-t and the GARCH-t are typical, with a small degree of freedom in the t-distribution and strong persistence measures of ϕ and $\beta_1 + \beta_2$ in volatility. The exception is for the SV-t applied to IP Growth, where there is a larger degree of freedom parameter. In this case the fat-tails are generated through the log-volatility, which has a much larger σ_v^2 than the other data.

Figure 2 shows the posterior mean of the variance components for the SV-IHMM model that is applied to AAPL for the period 2012 to 2020. As discussed earlier, the h_t process by construction captures the smooth changes in the volatility. Deviations from this are controlled by ω_{s_t} , which captures the local unconditional mean of the log-volatility, and as the bottom plot shows, is much more transitory in nature than h_t . This allows for a volatility shock with little to no persistence, where abrupt breaks are captured by ω_{s_t} and we avoid the problem that is common to standard GARCH and SV models, in which the effects of large volatility shocks last too long (Mikosch and Stărică, 2004; Stărică and Granger, 2005).

9 Out-of-Sample Forecasts

We perform recursive one-period ahead out-of-sample forecasts by using each of the models. Two measurement are computed. We report the log-predictive likelihood (LPL), which evaluates the predictive accuracy of the entire predictive distribution. The second measure is root-mean squared forecast error (RMSFE) of the predictive mean.

Table 3 shows the LPL, the log-Bayes factor in favour of the SV-IHMM against the benchmarks, and the RMSFE among all of the models for the four datasets. We consider a large out-of-sample period with which to compare the models. In this paper, the training sample is set to approximately the first five-year data, and the out-of-sample period starts from the closest beginning of a calendar year. For example, the out-of-sample size is 8,823 observations for AAPL, 10,856 observations for USD/CAD, 7,543 observations for Crude Oil, and 1,164 observations for IP Growth. To compute the forecasts, each model is re-estimated in each out-of-sample period.

There are several points worth mentioning. First, the SV-IHMM provides the best forecast results compared to all of the benchmark models in terms of density forecasts. This model also has a positive log-Bayes factor against all competitors. The SV-DPM specification is the second-best model and is always superior to or marginally better than the SV-t. Third, the GARCH-t is quite competitive and is better than the SV-t for IP Growth. The fat tails of the SV-t are always preferred to the SV-N except for the case of IP Growth where the two models predict equally well. The SV-N does produce fat tails in the predictive density but the generally small degree of freedom of the parameter estimates in the SV-t (see Table 2) indicate that this is insufficient. The SV-DPM and SV-IHMM capture the non-Gaussian fat tails through a discrete mixture of distributions.

Although the evidence for the SV-IHMM is very strong over the SV-DPM we acknowledge that the out-of-sample period is very large. This means that it takes a significant amount of data to uncover the gains the SV-IHMM has over the SV-DPM. The key difference in these models is the Markov chain structure governing the states in the SV-IHMM. Finally, the differences in RMSFE are very minor across models.

Some differences in the models can be seen in Figure 3 which shows log-predictive densities for various dates. Generally, when necessary, the SV-IHMM can produce thicker tails than the SV-DPM model.

9.1 Cumulative Log-Bayes Factors

Some insight into model performance is seen in Figure 4, which plots the cumulative log-BF between the SV-IHMM and other top performing benchmark models at each point in time.

If the curve is sloping upward (downward), this indicates the SV-IHMM does better (worse) in accounting for the associated realized data at time t .

Overall, each of the plots shows gradually increasing log-Bayes factors in support of the SV-IHMM. None of the results of the final log-Bayes factors are driven by a few influential outliers and, instead, come from consistent gains over the out-of-sample period. The SV-IHMM can take some time to show improvements over the SV-DPM in the case of Crude Oil and IP Growth. This is likely due to needing more data to learn about the more complex transition matrix here.

10 Robustness

The hierarchical prior in the SV-IHMM automatically provides some robustness to prior settings, but the priors on the precision parameters η and α are informative. This is standard and necessary, as it imposes some weak structure on density estimation. Broadly speaking these parameters control the number of active states in the model and, as such, govern parsimony. To explore their impact on the results, we report the posterior estimates for the full sample and we recompute the out-of-sample forecasts for a loose prior for $\eta \sim \text{Gamma}(5, 5)$ and $\alpha \sim \text{Gamma}(5, 5)$ and a tight prior for $\eta \sim \text{Gamma}(0.5, 8)$ and $\alpha \sim \text{Gamma}(0.5, 8)$.

Table 4 compares the results of two different prior settings. The posterior estimates of the SV component are very similar over all prior settings but more states are used on average for the loose prior as expected. The loose prior tends to reduce the LPL in the USD/CAD application while it improves in IP Growth. The tighter prior does not show significant changes in LPL with respect to benchmark prior. For AAPL and Crude Oil, the alternative priors have a small impact on LPL and RMSFE.

11 Conclusion

This paper proposes a new Bayesian semiparametric stochastic volatility model with Markovian mixtures. The model nests the SV-DPM model proposed by Jensen and Maheu (2010) but allows the unknown innovation distribution to change over time. The empirical results show that this change is important. In general, the SV-IHMM consistently outperforms all of the benchmark models in terms of out-of-sample density forecasts. The results for the SV-IHMM are robust to different prior settings.

References

- Antoniak, C. E. (1974). Mixtures of Dirichlet processes with applications to Bayesian non-parametric problems. *The Annals of Statistics*, 2(6):1152–1174.
- Bauwens, L., Dufays, A., and Rombouts, J. V. K. (2014). Marginal likelihood computation for Markov switching and change-point GARCH models. *Journal of Econometrics*, Volume 178, Issue P3:508–522.
- Bollerslev, T. (1986). Generalized autoregressive conditional heteroskedasticity. *Journal of Econometrics*, 31(3):307–327.
- Calvet, L. E. and Fisher, A. J. (2004). How to forecast long-run volatility: Regime switching and the estimation of multifractal processes. *Journal of Financial Econometrics*, 2(1):49–83.
- Carriero, A., Clark, T. E., and Marcellino, M. (2019). Large Bayesian vector autoregressions with stochastic volatility and non-conjugate priors. *Journal of Econometrics*, 212(1):137–154.
- Chan, J. (2013). Moving average stochastic volatility models with application to inflation forecast. *Journal of Econometrics*, 176(2):162–172.
- Chan, J. C. (2017). The stochastic volatility in mean model with time-varying parameters: An application to inflation modeling. *Journal of Business & Economic Statistics*, 35(1):17–28.
- Chib, S. (1996). Calculating posterior distributions and modal estimates in Markov mixture models. *Journal of Econometrics*, 75(1):79–97.
- Delatola, E.-I. and Griffin, J. E. (2011). Bayesian nonparametric modelling of the return distribution with stochastic volatility. *Bayesian Analysis*, 6(4):901–926.
- Delatola, E.-I. and Griffin, J. E. (2013). A Bayesian semiparametric model for volatility with a leverage effect. *Computational Statistics & Data Analysis*, 60:97–110.
- Diebold, F. X., Schorfheide, F., and Shin, M. (2017). Real-time forecast evaluation of DSGE models with stochastic volatility. *Journal of Econometrics*, 201(2):322–332.
- Dufays, A. (2016). Infinite-state Markov-switching for dynamic volatility. *Journal of Financial Econometrics*, 14(2):418–460.

- Fox, E. B., Sudderth, E. B., Jordan, M. I., and Willsky, A. S. (2011). A sticky HDP-HMM with application to speaker diarization. *The Annals of Applied Statistics*, pages 1020–1056.
- Griffin, J. and Steel, M. (2011). Stick-breaking autoregressive processes. *Journal of Econometrics*, 162(2):383–396.
- Hou, C. (2017). Infinite hidden Markov switching VARs with application to macroeconomic forecast. *International Journal of Forecasting*, 33(4):1025–1043.
- Jensen, M. J. and Maheu, J. M. (2010). Bayesian semiparametric stochastic volatility modeling. *Journal of Econometrics*, 157(2):306–316.
- Jin, X. and Maheu, J. M. (2016). Bayesian semiparametric modeling of realized covariance matrices. *Journal of Econometrics*, 192(1):19–39.
- Jin, X., Maheu, J. M., and Yang, Q. (2019). Bayesian parametric and semiparametric factor models for large realized covariance matrices. *Journal of Applied Econometrics*.
- Jin, X., Maheu, J. M., and Yang, Q. (2021). Infinite Markov pooling of predictive distributions. *Journal of Econometrics*, forthcoming.
- Jochmann, M. (2015). Modeling U.S. inflation dynamics: A Bayesian nonparametric approach. *Econometric Reviews*, 34(5):537–558.
- Kalli, M., Walker, S. G., and Damien, P. (2013). Modeling the conditional distribution of daily stock index returns: An alternative Bayesian semiparametric model. *Journal of Business & Economic Statistics*, 31(4):371–383.
- Liu, J. (2020). A Bayesian semiparametric realized stochastic volatility model. *Journal of Risk and Financial Management*, 14.
- Maheu, J. M. and McCurdy, T. H. (2000). Volatility dynamics under duration-dependent mixing. *Journal of Empirical Finance*, 7(3-4):345–372.
- Maheu, J. M. and Yang, Q. (2016). An infinite hidden Markov model for short-term interest rates. *Journal of Empirical Finance*, 38:202–220.
- Marcellino, M., Porqueddu, M., and Venditti, F. (2016). Short-term GDP forecasting with a mixed-frequency dynamic factor model with stochastic volatility. *Journal of Business & Economic Statistics*, 34(1):118–127.

- Mikosch, T. and Stărică, C. (2004). Nonstationarities in financial time series, the long-range dependence, and the IGARCH effects. *The Review of Economics and Statistics*, 86(1):378–390.
- Ryden, T., Terasvirta, T., and Asbrink, S. (1998). Stylized facts of daily return series and the hidden Markov model. *Journal of Applied Econometrics*, 13(3):217–244.
- Sethuraman, J. (1994). A constructive definition of Dirichlet priors. *Statistica Sinica*, pages 639–650.
- Song, Y. (2014). Modelling regime switching and structural breaks with an infinite hidden Markov model. *Journal of Applied Econometrics*, 29(5):825–842.
- Stărică, C. and Granger, C. (2005). Nonstationarities in stock returns. *The Review of Economics and Statistics*, 87(3):503–522.
- Taylor, S. J. (1982). Financial returns modelled by the product of two stochastic processes – a study of the daily sugar prices 1961-75. *Time Series Analysis: Theory and Practice*, 1:203–226.
- Teh, Y. W., Jordan, M. I., Beal, M. J., and Blei, D. M. (2006). Hierarchical Dirichlet processes. *Journal of the American Statistical Association*, 101(476):1566–1581.
- Van Gael, J., Saatci, Y., Teh, Y. W., and Ghahramani, Z. (2008). Beam sampling for the infinite hidden Markov model. In *Proceedings of the 25th International Conference on Machine Learning*, pages 1088–1095. ACM.
- Virbickaitė, A. and Lopes, H. F. (2018). Bayesian semiparametric Markov switching stochastic volatility model. *Applied Stochastic Models in Business and Industry*.
- Yang, Q. (2019). Stock returns and real growth: A Bayesian nonparametric approach. *Journal of Empirical Finance*, 38:202–220.

Table 1: Descriptive Statistics

Returns	Mean	Median	StDev	Skewness	Ex.Kurtosis	Min	Max
AAPL	0.0711	0.0000	2.9081	-1.7501	46.5407	-73.1248	28.6890
USD/CAD	-0.0006	0.0000	0.4087	0.1098	10.1554	-3.8070	5.0716
Crude Oil	-0.0117	-0.0213	2.5514	1.8373	69.8919	-41.2023	64.3699
IP Growth	0.2493	0.2800	1.9409	-0.0607	12.8184	-14.6100	15.3219

Table 2: Posterior Summary of Parameters

Panel A: AAPL

	SV-IHMM		SV-DPM		SV-t		GARCH-t	
	Mean	0.95 DI	Mean	0.95 DI	Mean	0.95 DI	Mean	0.95 DI
μ					0.1188	(0.0816, 0.1559)		0.1417 (0.1239, 0.1563)
ξ					0.0122	(0.0067, 0.0188)	β_0	0.0260 (0.0139, 0.0404)
ϕ	0.9993	(0.9985, 0.9999)	0.9928	(0.9888, 0.9962)	0.9909	(0.9864, 0.9947)	β_2	0.9332 (0.9217, 0.9461)
σ_ν^2	0.0011	(0.0007, 0.0017)	0.0098	(0.0058, 0.0147)	0.0122	(0.0078, 0.0182)	β_1	0.0394 (0.0324, 0.0452)
ν					6.1802	(5.5081, 6.9721)		5.2532 (4.9630, 5.4631)
α	1.2308	(0.7548, 1.8503)						
η	0.9454	(0.4342, 1.6495)	0.4132	(0.1180, 0.8610)				
K	10.3052	(8.0000,13.0000)	6.1295	(3.0000,10.0000)				

Panel B: USD/CAD

	SV-IHMM		SV-DPM		SV-t		GARCH-t	
	Mean	0.95 DI	Mean	0.95 DI	Mean	0.95 DI	Mean	0.95 DI
μ					-0.0001	(-0.0038, 0.0035)		-0.0005 (-0.0043, 0.0031)
ξ					-0.0127	(-0.0189,-0.0069)	β_0	0.0001 (0.0000, 0.0002)
ϕ	0.9993	(0.9987, 0.9998)	0.9962	(0.9943, 0.9979)	0.9951	(0.9929, 0.9971)	β_2	0.9268 (0.9173, 0.9351)
σ_ν^2	0.0024	(0.0015, 0.0033)	0.0116	(0.0091, 0.0148)	0.0132	(0.0100, 0.0174)	β_1	0.0542 (0.0473, 0.0620)
ν					10.0817	(8.2735,12.5834)		6.3324 (5.6626, 7.0463)
α	0.6543	(0.3615, 1.0422)						
η	1.0455	(0.4979, 1.8023)	0.3647	(0.1060, 0.7685)				
K	10.9187	(9.0000,14.0000)	5.3633	(3.0000, 9.0000)				

Panel C: Crude Oil

	SV-IHMM		SV-DPM		SV-t		GARCH-t	
	Mean	0.95 DI	Mean	0.95 DI	Mean	0.95 DI	Mean	0.95 DI
μ					-0.0594	(-0.0965,-0.0227)		-0.0754 (-0.0995,-0.0484)
ξ					0.0148	(0.0091, 0.0214)	β_0	0.0488 (0.0337, 0.0657)
ϕ	0.9933	(0.9901, 0.9961)	0.9893	(0.9851, 0.9931)	0.9875	(0.9826, 0.9916)	β_2	0.9068 (0.8920, 0.9197)
σ_ν^2	0.0098	(0.0066, 0.0137)	0.0164	(0.0120, 0.0214)	0.0182	(0.0139, 0.0237)	β_1	0.0525 (0.0448, 0.0622)
ν					8.9162	(7.4014,10.9299)		5.1749 (4.8852, 5.7158)
α	1.5493	(0.8461, 2.4802)						
η	0.5526	(0.1694, 1.2078)	0.4203	(0.1155, 0.9213)				
K	5.6379	(4.0000,10.0000)	6.1468	(3.0000,12.0000)				

Panel D: IP Growth

	SV-IHMM		SV-DPM		SV-t		GARCH-t	
	Mean	0.95 DI	Mean	0.95 DI	Mean	0.95 DI	Mean	0.95 DI
μ					0.1411	(0.0956, 0.1869)		0.1631 (0.1183, 0.2040)
ρ					0.4158	(0.3576, 0.4734)		0.3973 (0.3466, 0.4574)
ξ					-0.0098	(-0.0335, 0.0118)	β_0	0.0521 (0.0249, 0.0825)
ϕ	0.9966	(0.9941, 0.9990)	0.9970	(0.9948, 0.9992)	0.9622	(0.9354, 0.9866)	β_2	0.5993 (0.4912, 0.7464)
σ_ν^2	0.0017	(0.0006, 0.0046)	0.0020	(0.0008, 0.0039)	0.1411	(0.0518, 0.2265)	β_1	0.2400 (0.1466, 0.3233)
ν					24.6920	(6.1601,48.5491)		4.5288 (3.5544, 5.5427)
α	1.2772	(0.7094, 2.1243)						
η	0.6872	(0.2446, 1.3464)	0.5785	(0.2191, 1.1131)				
K	6.9515	(5.0000,11.0000)	7.6072	(5.0000,11.0000)				

Note 1: ρ denotes the parameter of the additional AR(1) term for each model.

Note 2: μ , ρ and ξ are state-dependent parameters for SV-IHMM and SV-DPM.

Note 3: β_0 , β_1 and β_2 are the GARCH parameters from (7).

Table 3: Out-of-Sample Forecast Performance

	AAPL			USD/CAD		
	LPL	log BF	RMSFE	LPL	log BF	RMSFE
SV-IHMM	-19846.89	—	2.8373	-3581.02	—	0.4283
SV-DPM	-19893.40	46.5087	2.8341	-3616.36	35.3434	0.4284
SV-t	-19892.58	45.6890	2.8345	-3629.96	48.9389	0.4284
GARCH-t	-19953.12	106.2377	2.8347	-3636.74	55.7248	0.4284
IHMM	-19934.70	87.8154	2.8382	-3716.15	135.1321	0.4297
SV-N	-20037.88	190.9949	2.8350	-3688.19	107.1708	0.4284
GARCH-N	-20542.51	695.6251	2.8343	-3914.81	333.7918	0.4284
	Crude Oil			IP Growth		
	LPL	log BF	RMSFE	LPL	log BF	RMSFE
SV-IHMM	-16189.88	—	2.6687	-1622.73	—	1.6058
SV-DPM	-16213.17	23.2905	2.6688	-1641.43	18.6986	1.5835
SV-t	-16221.76	31.8723	2.6690	-1661.11	38.3765	1.5823
GARCH-t	-16226.84	36.9565	2.6689	-1649.76	27.0263	1.5808
IHMM	-16231.72	41.8338	2.6706	-1635.47	12.7412	1.5903
SV-N	-17019.77	829.8850	2.6687	-1662.67	39.9405	1.5805
GARCH-N	-16492.99	303.1089	2.6688	-1791.79	169.0626	1.5837

Note 1: The number of out-of-sample observations for AAPL, USD/CAD, Crude Oil and IP Growth are 8823, 10856, 7543 and 1164, respectively.

Note 2: The log Bayes factors are the difference between the log-predictive likelihoods of the SV-IHMM model and each corresponding model.

Table 4: Robustness: Posterior Estimates and Forecast Performance

AAPL							
	ϕ	σ_v^2	α	η	K	LPL	RMSFE
Loose	0.9989	0.0014	3.3395	1.8419	13.1340	-19843.27	2.8373
Benchmark	0.9993	0.0011	1.2308	0.9454	10.3052	-19846.89	2.8373
Tight	0.9990	0.0011	0.7743	0.8449	10.4248	-19843.70	2.8379
USD/CAD							
	ϕ	σ_v^2	α	η	K	LPL	RMSFE
Loose	0.9994	0.0015	1.2870	2.3436	16.3146	-3591.81	0.4283
Benchmark	0.9993	0.0024	0.6543	1.0455	10.9187	-3581.02	0.4283
Tight	0.9991	0.0023	0.6986	0.7403	9.0708	-3577.30	0.4283
Crude Oil							
	ϕ	σ_v^2	α	η	K	LPL	RMSFE
Loose	0.9932	0.0099	3.6505	1.1750	6.9398	-16190.03	2.6695
Benchmark	0.9933	0.0098	1.5493	0.5526	5.6379	-16189.88	2.6687
Tight	0.9938	0.0081	1.5841	0.3766	5.0579	-16192.12	2.6691
IP Growth							
	ϕ	σ_v^2	α	η	K	LPL	RMSFE
Loose	0.9964	0.0014	2.1213	1.5240	8.8890	-1616.03	1.6060
Benchmark	0.9966	0.0017	1.2772	0.6872	6.9515	-1622.73	1.6058
Tight	0.9964	0.0014	1.0268	0.4840	6.1176	-1624.92	1.6075

Note 1: This table reports posterior mean estimates for ϕ , σ_v^2 , α , η and K , in addition to out-of-sample LPL and RMSFE using the same out-of-sample period as before.

Note 2: The loose prior represents $Gamma(5, 5)$; the benchmark prior represents $Gamma(2, 8)$; and the tight prior represents $Gamma(0.5, 8)$.

Figure 1: Posterior Histogram of Number of Active States

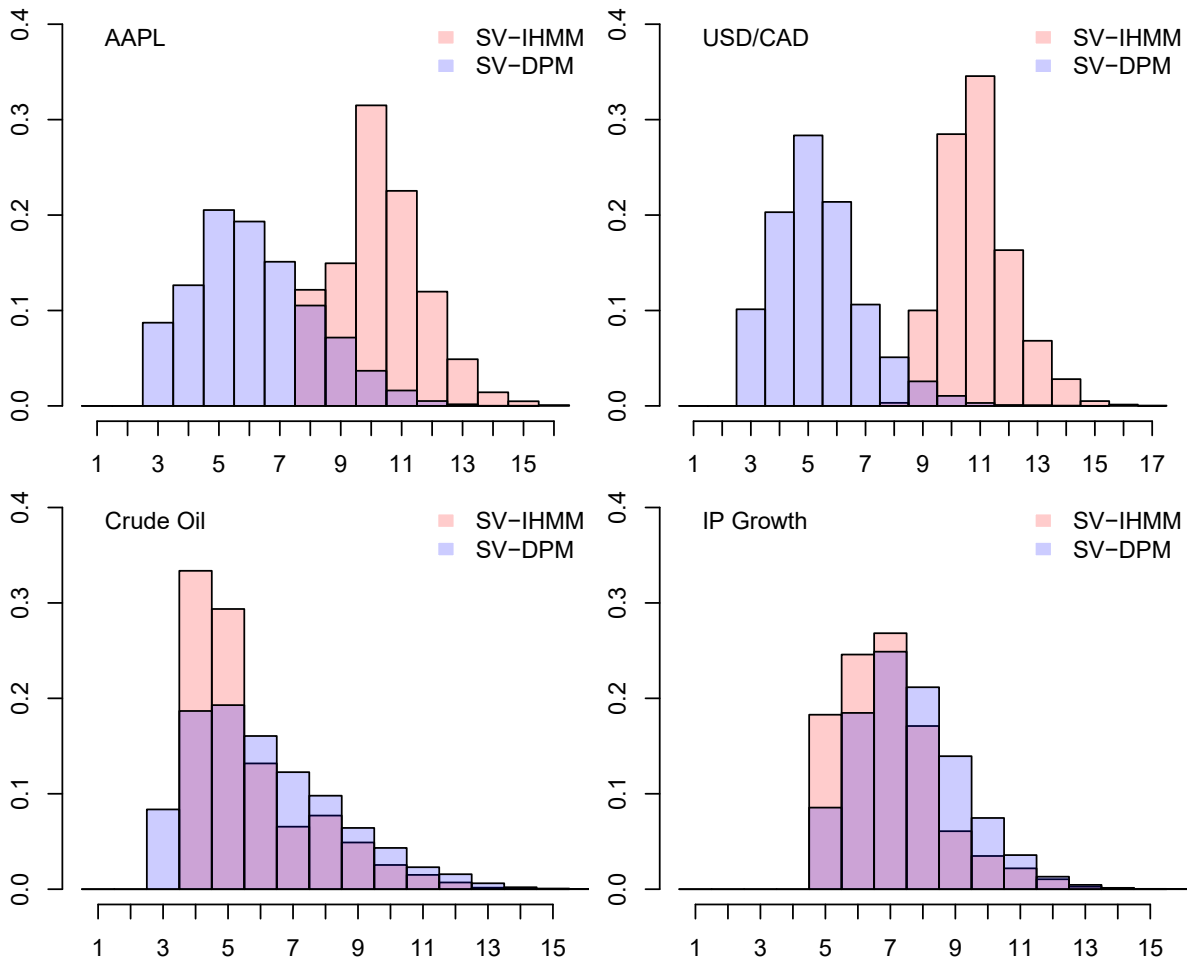


Figure 2: AAPL Application: Posterior Mean of Variance Components

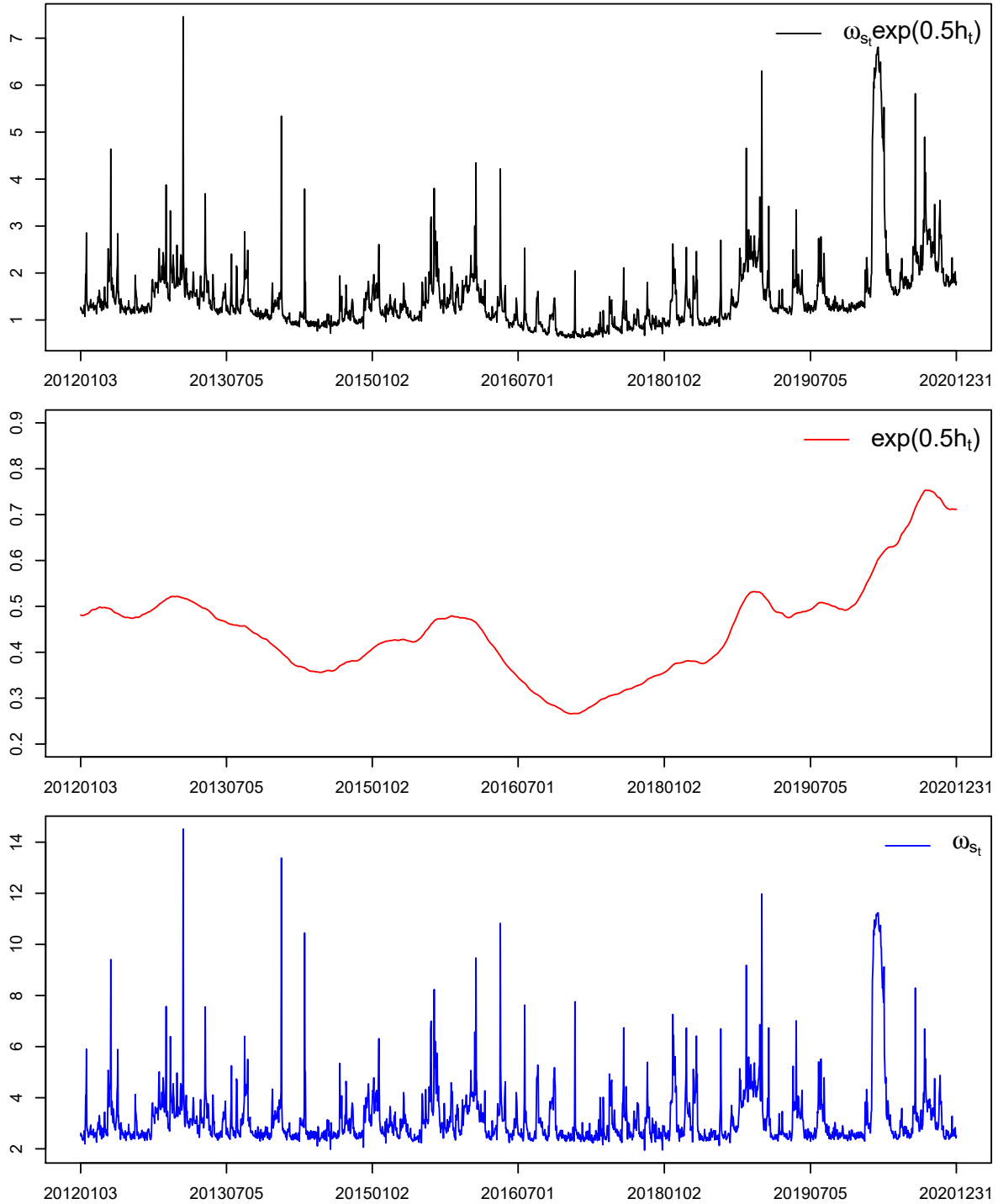


Figure 3: Log-Predictive Densities at Selected Dates

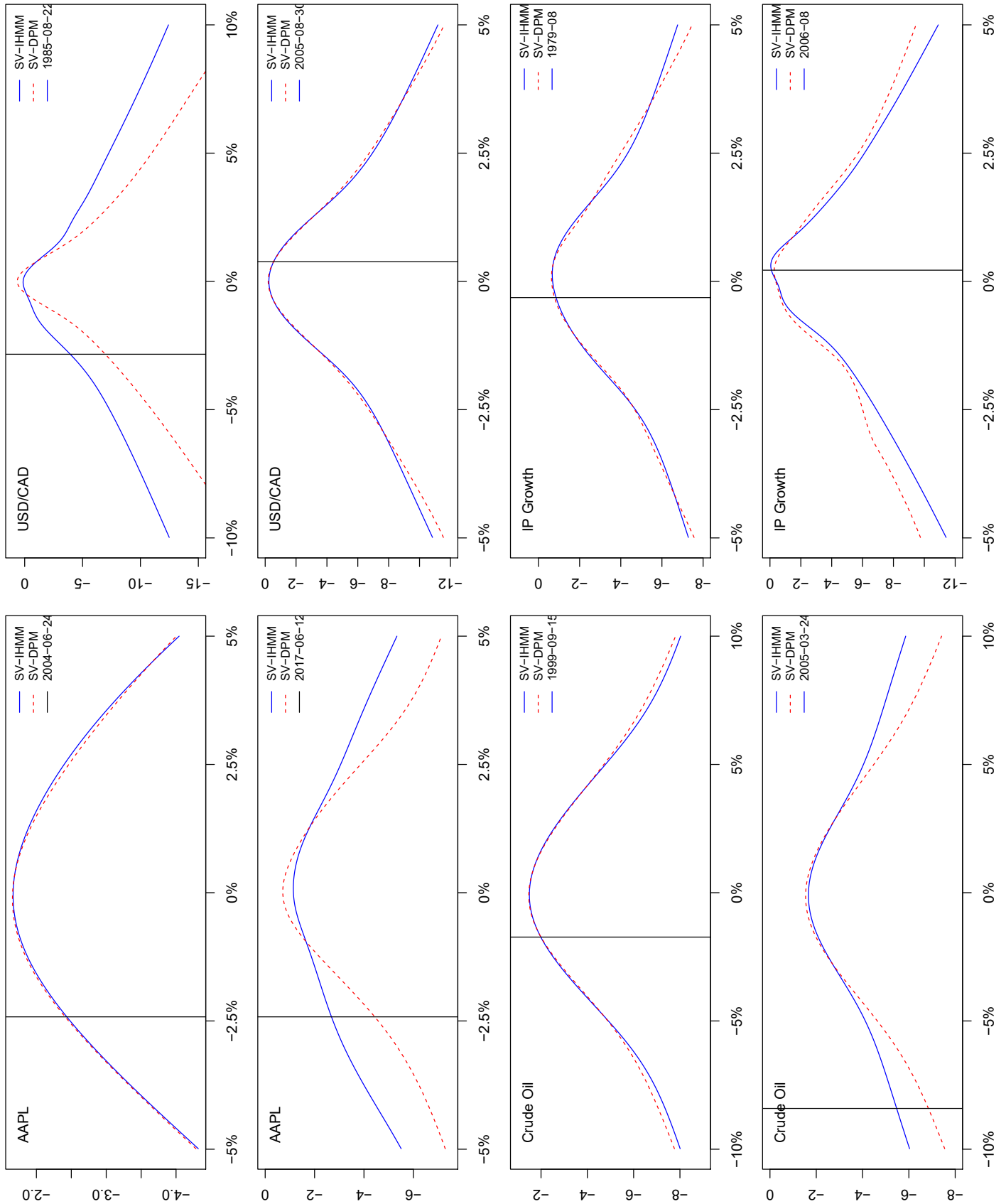
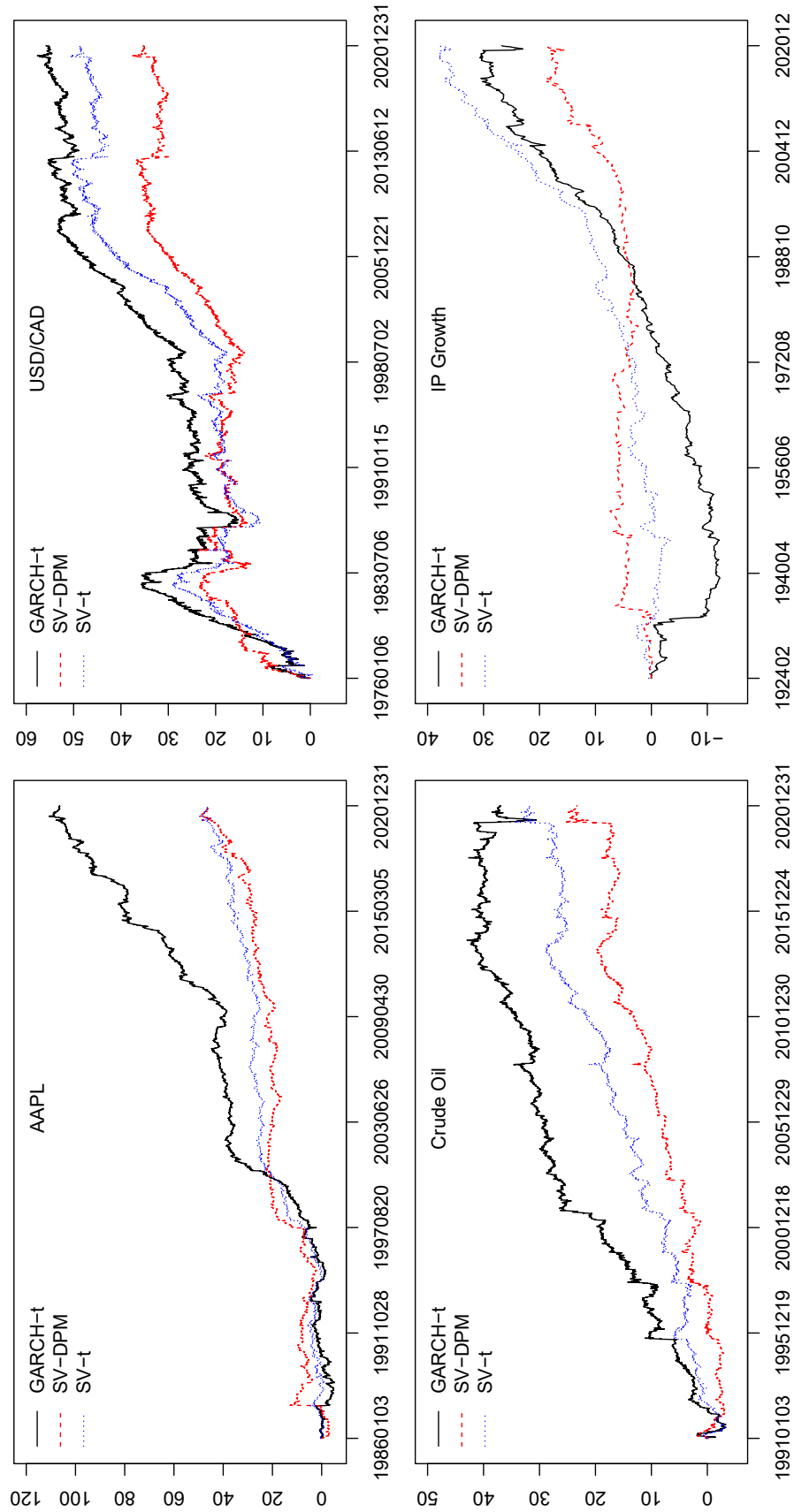


Figure 4: Cumulative Log-Bayes Factor for SV-IHMM



A Appendix: Posterior Sampling Steps for SV-IHMM

1. We sample $u_{1:T}|\Gamma, \Pi$: The auxiliary slice variable $U = \{u_t\}_{t=1}^T$ is drawn from $u_1 \sim U(0, \gamma_{s_1})$ and $u_t \sim U(0, \pi_{s_{t-1}s_t})$.
2. We update K . Similar to DPM model, if K does not meet the following condition

$$\min \{u_t\}_{t=1}^T > \max \{\pi_{jR}\}_{j=1}^K \quad (24)$$

then K needs to be increased by 1 ($K' = K + 1$), and all of the parameters need to be drawn from the base measure. In addition, since a new ‘‘major’’ state is introduced, Γ and Π also need to be updated accordingly:

- (a) $\Theta_{K'} \sim H$;
- (b) We draw $v \sim \text{Beta}(1, \eta)$, then we update $\Gamma = (\gamma_1, \dots, \gamma_K, \gamma_{K'}, \gamma_R)'$, where $\gamma_{K'} = v\gamma_R$ and $\gamma_R = (1 - v)\gamma_R$;
- (c) We draw $v_j \sim \text{Beta}(\alpha\gamma_{K'}, \alpha\gamma_R)$, then we update $\Pi_j = (\pi_{j1}, \dots, \pi_{jK}, \pi_{jK'}, \pi_{jR})$ for $j = 1, \dots, K$, where $\pi_{jK'} = v\pi_{jR}$ and $\pi_{jR} = (1 - v)\pi_{jR}$;
- (d) We draw the K' th row of Π , $\Pi_{K'}$, by $\Pi_{K'} \sim \text{Dir}(\alpha\gamma_1, \dots, \alpha\gamma_K, \alpha\gamma_{K'}, \alpha\gamma_R)$.

The above steps are repeated until inequality (24) holds.

3. The forward filter for $s_{1:T}|r_{1:T}, u_{1:T}, \Gamma, \Pi, \Theta, h_{1:T}$. Iterating the following steps forward from 1 to T , we have the following:
 - (a) The prediction step for initial state s_1 is as follows:

$$p(s_1 = k|u_1, \Gamma) \propto \mathbb{1}(u_1 < \gamma_k), \quad k = 1, \dots, K \quad (25)$$

for the following states $s_{2:T}$:

$$p(s_t = k|r_{1:t-1}, u_{1:t}, \Pi, \Theta, h_{1:t-1}) \propto \sum_{j=1}^K \mathbb{1}(u_t < \pi_{jk}) p(s_{t-1} = j|r_{1:t-1}, u_{1:t-1}, \Pi, \Theta, h_{1:t-1}) \quad (26)$$

- (b) We update the step for $s_{1:T}$:

$$p(s_t = k|r_{1:t}, u_{1:t}, \Pi, \Theta, h_{1:t}) \propto p(r_t|r_{t-1}, \theta_k, h_t) p(s_t = k|r_{1:t-1}, u_{1:t}, \Pi, \Theta, h_{1:t-1}) \quad (27)$$

4. The backward sampler for $s_{1:T}|r_{1:T}, u_{1:T}, \Pi, \Theta, h_{1:T}$. We sample states $s_{1:T}$ using the previously filtered values backward from T to 1:

- (a) for the terminal state s_T , we sample directly from $p(s_T|r_{1:T}, u_{1:T}, \Pi, \Theta, h_{1:T})$
- (b) for the rest states, we sample from the following,

$$p(s_t = k|s_{t+1} = j, r_{1:t}, u_{1:t+1}, \Pi, \Theta, h_{1:T}) \propto \mathbb{1}(u_{t+1} < \pi_{kj}) p(s_t = k|r_{1:t}, u_{1:t}, \Pi, \Theta, h_{1:T}) \quad (28)$$

5. Sample $c_{1:K}|s_{1:T}, \Gamma, \alpha$. Following the sampling approach of Fox et al. (2011), we perform the following:

- (a) We count the number of each transition type, n_{jk} , number of times state j switches to state k .
- (b) We simulate an auxiliary trial variable $x_i \sim \text{Bernoulli}\left(\frac{\alpha\gamma_k}{i-1+\alpha\gamma_k}\right)$, for $i = 1, \dots, n_{jk}$. If the trial is successful, then an ‘‘oracle’’ urn step is involved at the i th step toward n_{jk} and we increase the corresponding ‘‘oracle’’ counts, o_{jk} , by one.
- (c) $c_k = \sum_{j=1}^K o_{jk}$.

6. Sample η : Following Fox et al. (2011) and Maheu and Yang (2016), we assume a Gamma prior $\eta \sim \text{Gamma}(a_1, b_1)$, and let $c = \sum_{j=1}^K c_j$,

- (a) $\nu \sim \text{Bernoulli}\left(\frac{c}{c+\eta}\right)$
- (b) $\lambda \sim \text{Beta}(\eta + 1, c)$
- (c) $\eta \sim \text{Gamma}(a_1 + K - \nu, b_1 - \log \lambda)$

7. Sample α : Following Fox et al. (2011), we assume a Gamma prior $\alpha \sim \text{Gamma}(a_2, b_2)$ and let $n_j = \sum_{k=1}^K n_{jk}$,

- (a) $\nu_j \sim \text{Bernoulli}\left(\frac{n_j}{n_j+\alpha}\right)$
- (b) $\lambda_j \sim \text{Beta}(\alpha + 1, n_j)$
- (c) $\alpha \sim \text{Gamma}\left(a_2 + c - \sum_{j=1}^K \nu_j, b_2 - \sum_{j=1}^K \log(\lambda_j)\right)$

8. Sample $\Gamma|c_{1:K}, \eta$: Given the ‘‘oracle’’ urn counts $c_{1:K}$ and the property of Dirichlet process, the conjugate posterior is

$$\Gamma|c_{1:K}, \eta \sim \text{Dir}(c_1, \dots, c_K, \eta) \quad (29)$$

9. Sample $\Pi|n_{1:K}, \Gamma, \alpha$: Similarly, the conjugate posterior of Π_j is

$$\Pi_j|n_{j,1:K}, \Gamma, \alpha \sim \text{Dir}(\alpha\gamma_1 + n_{j1}, \dots, \alpha\gamma_K + n_{jK}, \alpha\gamma_R) \quad (30)$$

10. Sample $\Theta|r_{1:T}, s_{1:T}, h_{1:T}$. We define $Y_k \equiv \left(e^{-\frac{1}{2}h_t} r_t | s_t = k\right)_{t=2}^T$, and $X_k \equiv \left(e^{-\frac{1}{2}h_t} | s_t = k\right)_{t=2}^T$. The linear model is now

$$Y_k = X_k \mu_k + \omega_k \epsilon_k, \quad \epsilon_k \sim N(0, I) \quad (31)$$

The posteriors are

$$p(\mu_k | Y_k, \omega_k) \sim \prod_{t:s_t=k} p(r_t | \mu_k, \omega_k) p(\mu_k) \quad (32)$$

$$\sim N(M_\mu, V_\mu) \quad (33)$$

where

$$M_\mu = V_\mu (\omega_k^{-1} X_k' Y_k + B_0^{-1} b_0) \quad (34)$$

$$V_\mu = (\omega_k^{-1} X_k' X_k + B_0^{-1})^{-1} \quad (35)$$

and

$$p(\omega_k | Y, \mu_k) \propto \prod_{t:s_t=k} p(r_t | \mu_k, \omega_k) p(\omega_k) \quad (36)$$

$$\sim IG(\bar{v}, \bar{s}) \quad (37)$$

where

$$\bar{v} = \frac{T_k}{2} + v_0 = \frac{1}{2} \sum_{t=1}^T \mathbb{1}(s_t = k) + v_0 \quad (38)$$

$$\bar{s} = \frac{1}{2} (Y_k - X_k \mu_k)' (Y_k - X_k \mu_k) + s_0 \quad (39)$$

11. Sample hierarchical priors.

(a) Sample $b_0|\mu_{1:K}, B_0, h_0, H_0 \sim N(\mu_b, \Sigma_b)$, where

$$\mu_b = \Sigma_b \left(B_0^{-1} \sum_{k=1}^K \mu_k + H_0^{-1} h_0 \right) \quad (40)$$

$$\Sigma_b = (K B_0^{-1} + H_0^{-1})^{-1} \quad (41)$$

(b) Sample $B_0|\mu_{1:K}, b_0, a_0, A_0 \sim IW(\Omega_B, \omega_b)$, where

$$\omega_b = K + a_0 \quad (42)$$

$$\Omega_B = \sum_{k=1}^K (\mu_k - b_0)(\mu_k - b_0)' + A_0 \quad (43)$$

(c) Sample $s_0|\sigma_{1:K}^2, v_0, c_0, d_0 \sim Gamma(c_s, d_s)$, where

$$c_s = K v_0 + c_0 \quad (44)$$

$$d_s = \sum_{k=1}^K \sigma_k^{-2} + d_0 \quad (45)$$

(d) Sample $v_0|\sigma_{1:K}^2, s_0, g_0$. There IS no easily applicable conjugate prior for v_0 , so a Metropolis-Hastings step needs to be applied. We implement a Gamma proposal, following Maheu and Yang (2016):

$$v'_0|v_0 \sim Gamma\left(\tau, \frac{\tau}{v_0}\right) \quad (46)$$

and the acceptance rate is

$$\min \left\{ 1, \frac{p(v'_0|\sigma_{1:K}^2, s_0, g_0)/q(v'_0|v_0)}{p(v_0|\sigma_{1:K}^2, s_0, g_0)/q(v_0|v'_0)} \right\} \quad (47)$$

12. $\theta_h|h_{1:T}$: Equation (1d) is simply a linear regression model. Assuming conjugate prior $\beta \sim N(b_h, B_h)$, the posterior is

$$\delta|\sigma_v, h_{1:T} \sim N(M, V) \quad (48)$$

$$M = V \left(\sigma_v^{-2} \sum_{t=1}^{T-1} h_t h_{t+1}' + b_h B_h^{-1} \right) \quad (49)$$

$$V = \left(\sigma_v^{-2} \sum_{t=1}^{T-1} h_t h_t' + B_h^{-1} \right)^{-1} \quad (50)$$

Based on the above linear regression model with conjugate prior $\sigma_v^2 \sim IG(v_h, s_h)$, the posterior is

$$\sigma_v^2 | \delta, h_{1:T} \sim IG \left(\frac{T}{2} + v_h, \frac{\sum_{t=1}^{T-1} (h_{t+1} - \delta h_t)^2}{2} + s_h \right) \quad (51)$$

13. Sample $h_t | h_{-t}, r_{1:T}, \Theta, s_{1:T}$: We use the block Metropolis-Hastings (MH) sampler as in Jensen and Maheu (2010) with random block size $k = \text{Poisson}(\lambda_h) + 1$. The proposal density is derived by approximating the autoregressive coefficient to 1. This approximation provides an analytic inversion of the covariance matrix. We draw $h'_{(t,\tau)}$ from the following proposal density

$$g(h_{(t,\tau)} | \dots) = N(h_{(t,\tau)}; M_h - 0.5V_h(\iota - \tilde{y}), V_h) \quad (52)$$

where

$$\tilde{y}_i = \frac{(r_i - \mu_{s_i})^2}{\omega_{s_i}} \exp(-M_{h,i}) \quad (53)$$

$$M_{h,i} = \frac{(k+1-i)h_{t-1} + ih_{\tau+1}}{k+1}, \quad i = 1, 2, \dots, k \quad (54)$$

$$V_{h,ij} = \sigma_v^2 \frac{\min(i, j)(1+k) - ij}{k+1} \quad (55)$$

$$V_{h,ij}^{-1} = \begin{cases} 2\sigma_v^2 & i = j \\ -\sigma_v^2 & j = i \pm 1 \\ 0 & \text{otherwise} \end{cases} \quad (56)$$

We accept $h'_{(t,\tau)}$ with probability

$$\min \left\{ 1, \frac{p(h'_{(t,\tau)} | r_{1:T}, h_{-(t,\tau)}, \Theta, s_{1:T}) / g(h'_{(t,\tau)} | h_{-(t,\tau)})}{p(h_{(t,\tau)} | r_{1:T}, h_{-(t,\tau)}, \Theta, s_{1:T}) / g(h_{(t,\tau)} | h_{-(t,\tau)})} \right\} \quad (57)$$